SUPERRESOLUTION SOURCE LOCALIZATION THROUGH DATA-ADAPTIVE REGULARIZATION

Dmitry M. Malioutov, Müjdat Çetin, John W. Fisher III, and Alan S. Willsky

Laboratory for Information and Decision Systems
Massachusetts Institute of Technology
77 Massachusetts Ave., Cambridge, MA 02139, USA

ABSTRACT

We address the task of source localization using a novel non-parametric data-adaptive approach based on regularized linear inverse problems with sparsity constraints. The class of penalty functions that we use for regularization favors sparsity of the reconstructions, thus producing superb resolution of the sources. We present a computationally efficient technique to carry out the numerical optimization of the resulting cost function. In comparison to conventional source localization methods, the proposed approach provides numerous improvements, including increased resolution, reduced sidelobes, and better robustness properties to noise, limited snapshots, and coherence of the sources. The method is developed for the general source localization scenario, encompassing nearfield and farfield, narrowband and broadband, and non-linear array geometry cases. Simulation results manifest the capabilities of the approach.

1. INTRODUCTION

Source localization using sensor arrays has been an active research area, playing a fundamental role in many applications involving electromagnetic, acoustic, and seismic sensing. Conventional beamformers have a limited resolution, and this has led to the development and successful application of more advanced techniques. Examples are Capon's minimum variance method [1], and a variety of superresolution methods based on eigenvalue decomposition, such as MUSIC [2]. Such methods exploit the presence of a *small* number of sources in order to focus the estimated signal energy towards the source locations to achieve superresolution.

We propose a different approach which exploits such sparse structure to a greater degree to achieve superresolution in source localization. We turn to the linear inverse problem framework for the relative ease with which prior information about the unknown quantity (signal energy as a function of location) can be incorporated into the model. To free the forward operator (the array steering matrix) from depending on the source locations, an overcomplete representation is used, which plays an important role in achieving sparsity. The key to the method is to use a non-quadratic sparsity-enforcing term such as an ℓ_p-quasi-norm in the cost function in conjunction with a least squares data-fidelity term. The source position estimate is obtained by forming the energy spectrum of the solution, and locating its peaks. In the past decade, related ideas have found use in various applications such as image restoration [4], radar imaging [5], and penalized regression [15]. There has also been some limited investigation of ideas similar to ours in the array processing literature [6, 7, 16]. In [14], we have presented a specific version of our proposed approach for the narrowband, farfield, uniform linear array (ULA) case. The contribution of the current paper is the extension of the framework to more general source localization scenarios.

Our experimental analysis on simulated data demonstrates that compared to methods such as MUSIC, the proposed technique offers increased resolution, reduced sidelobes, as well as robustness to noise, limited data, coherence of the sources, and to mismatch of the location of the sources with the scanning grid.

2. OBSERVATION MODEL

Consider K signals $u_k(t), k \in \{1, ..., K\}$, impinging on an array of M omnidirectional sensors corrupted by additive noise $n_m(t)$ resulting in sensor outputs $y_m(t), m \in \{1, ..., M\}$. Let $\{\theta_1, ..., \theta_{N_\theta}\}$ be a sampling grid of all source locations. In the farfield case, θ_n's are scalars representing the directions of arrival (DOA), whereas in the nearfield case, θ_n's are vectors containing range and bearing information. We represent the signal field by an $N_\theta \times 1$ vector $\mathbf{s}(t)$, where the n-th element $\mathbf{s}_n(t)$ is non-zero and equal to $u_k(t)$ if source k comes from θ_n, for some k. In the frequency domain, signal field at frequency ω will be denoted by $\mathbf{s}(\omega)$, resulting in a slight abuse of notation. Similarly, $\mathbf{n}(\omega)$ will be used for noise. In the narrowband case, the model becomes:

$$\mathbf{y}(t) = \mathbf{A}\mathbf{s}(t) + \mathbf{n}(t), \quad t = 1..T, \tag{1}$$

where $\mathbf{A} = \mathbf{A}(\omega_0)$ and ω_0 is the center frequency. For wideband case,

$$\mathbf{y}(\omega) = \mathbf{A}(\omega)\mathbf{s}(\omega) + \mathbf{n}(\omega), \quad \omega = \omega_1..\omega_W \tag{2}$$

The $M \times N_\theta$ matrices $\mathbf{A}(\omega)$ are composed of steering vectors corresponding to each potential source location. Unlike the narrowband case, in the wideband case the steering matrix is not the same for all snapshots, but rather it depends on frequency.

Note that $\mathbf{A}$ differs from the steering matrix representation used in many array processing methods in the sense that it contains steering vectors for *all* potential locations, rather than only the (unknown) source signal locations. Hence, in our framework $\mathbf{A}$ is known and does not depend on the actual source locations. The reason behind using such redundancy in the representation is our desire to formulate the problem in a sparse signal reconstruction framework. This can also be viewed as representing the ob-

servations as combination of elements from an overcomplete signal dictionary, as in adaptive signal representation methods such as basis pursuit [8].

In the nearfield case $\mathbf{A}$ also includes factors due to the uneven attenuation of the source signals at the sensors.

3. SOURCE LOCALIZATION SCHEME

As in numerous non-parametric source localization techniques, our approach consists of forming an estimate of the signal energy as a function of position, which ideally contains dominant peaks at the source locations. We need to obtain an estimate of the signal field $\mathbf{s}$ (hence its energy) through the sensor observations $\mathbf{y}$, which is in general an ill-posed inverse problem. The central idea in our approach is to solve this inverse problem via regularizing it by favoring sparse signal fields, where energy is concentrated around a small number of locations. In particular, we find $\mathbf{s}$ as the minimizer of an objective function of the following form: [1]

$$J(\mathbf{s}) = J_1(\mathbf{s}) + \alpha J_2(\mathbf{s}) \tag{3}$$

where $J_1(\mathbf{s})$ is an ℓ_2-norm-based data fidelity term, $J_2(\mathbf{s})$ reflects the regularizing sparsity constraint we would like to impose, and α is a scalar parameter controlling the tradeoff between data-fidelity and regularization. The choice of $J_2(\mathbf{s})$ is critical for attaining the objectives of superresolution and noise suppression. Some of the candidates include entropy [9], and ℓ_p-quasi-norm constraints. Note that the use of ℓ_2-norm in $J_2(\mathbf{s})$ leads to results proportional to the periodogram. The use of ℓ_1-norm is discussed in [16]. We use $J_2(\mathbf{s})$ based on ℓ_p-quasi-norms where $p < 1$. In simulation, we observe that keeping p strictly less than 1 noticeably increases resolution. Use of other non-quadratic functions is possible. Thus the objective function becomes:

$$J(\mathbf{s}) = \|\mathbf{y} - \mathbf{A}\mathbf{s}\|_2^2 + \alpha \|\mathbf{s}\|_p^p \tag{4}$$

where $\|\cdot\|_p$ denotes the ℓ_p-quasi-norm, $\left(\sum_i |s_i|^p\right)^{1/p}$.

Unlike some inverse problems applications such as image restoration, the data in sensor-array processing typically has one more dimension, time, which can be handled in numerous ways. The most direct way is to solve the inverse problem at each time instance (or at each frequency), and to use multiple reconstructions to get an estimate of the source locations. However, both the computational complexity and sensitivity to noise would be very high.

In the case when the complex envelopes are non-zero mean, averaging can be used to improve upon the previous case. The data is combined prior to the reconstructions, and thus only a single inverse problem has to be solved. The robustness to noise is also substantially improved. Finally, since the exact statistical nature of the sources plays a little role with such processing, only the means are of concern, so coherent sources can be readily handled.

Yet another possibility is to transform the data into the beamspace domain, and combine squared amplitudes of the time samples. The steered beams are sampled on a grid of angles, and the corresponding collection of manifold vectors is kept as columns in matrix $\mathbf{B}$. Then the beamspace data are

$$\mathbf{z}(t) = \mathbf{B}^H(\mathbf{y}(t) + \mathbf{n}(t)) = (\mathbf{B}^H\mathbf{A})\mathbf{s}(t) + \mathbf{B}^H\mathbf{n}(t) \tag{5}$$

[1]Note that we have suppressed the dependence on time t and frequency ω for simplicity.

Denote the i, j^{th} entry of $\mathbf{B}^H\mathbf{A}$ by $v_{i,j}$, and $\mathbf{B}^H\mathbf{n}(t)$ by $\tilde{\mathbf{n}}(t)$. Then

$$|z(t)|_i^2 = |\sum_j s_j(t)v_{i,j} + \tilde{n}_i(t)|^2$$

$$= \sum_j |s_j(t)|^2|v_{i,j}|^2 + 2\sum_{j_1 \neq j_2} s_{j_1}(t)^* s_{j_2}(t) v_{i,j_1}^* v_{i,j_2}$$

$$+ 2\sum_j s_j(t)^* v_{i,j}^* \tilde{n}_i(t) + |\tilde{n}_i(t)|^2$$

When the sources are uncorrelated and zero mean, and the noise is zero mean, the cross terms are all zero mean, and their time sums are negligible. Hence the average squared beamspace data $\overline{|\mathbf{z}|^2}$ can be represented well by a linear transformation of the element-by-element square of $\mathbf{B}^H\mathbf{A}$, denoted by $\mathbf{V}$, with average squared noise $\overline{|\tilde{\mathbf{n}}|^2}$ added.

$$\overline{|\mathbf{z}|^2} = \mathbf{V}\overline{|\mathbf{s}|^2} + \overline{|\tilde{\mathbf{n}}|^2} \tag{6}$$

Despite the assumptions of zero-mean and uncorrelatedness in the development, on simulated examples the reconstructions exhibit peaks in the vicinity of the correct source locations even when these conditions are not met.

3.1. Numerical Solution

Herein, we outline the solution of the optimization problem in (4). The sparsity enforcing matrix inversion algorithm applies with minor changes to all the three scenarios of treating time dependence, thus only the general form will be presented. In the beamspace and time-average versions it is applied once, whereas when the temporal data is not combined, it is applied for each snapshot.

In order to avoid dealing with nonsmooth optimization, we use the following smooth approximation to the ℓ_p-quasi-norm in (4) [3]:

$$\|\mathbf{s}\|_p^p \approx \sum_{i=1}^K (|\mathbf{s}_i|^2 + \epsilon)^{p/2} \tag{7}$$

where $\epsilon \geq 0$ is a small constant, K is the length of the complex vector $\mathbf{z}$, and $\mathbf{z}_i$ denotes its i-th element. The following slightly modified cost function ensues:

$$J_\epsilon(\mathbf{s}) = \|\mathbf{y} - \mathbf{A}\mathbf{s}\|_2^2 + \alpha \sum_{i=1}^{N_\theta} (|\mathbf{s}_i|^2 + \epsilon)^{p/2} \tag{8}$$

Note that $J_\epsilon(\mathbf{s}) \to J(\mathbf{s})$ as $\epsilon \to 0$. The minimization of $J(\mathbf{s})$ or $J_\epsilon(\mathbf{s})$ does not yield a closed-form solution in general, so numerical optimization techniques must be used.

For solution of this optimization problem, we use the half-quadratic regularization method of [11]. Half-quadratic regularization converts a non-quadratic optimization problem into a series of quadratic problems. We skip the derivations here and present the resulting iterative algorithm:

$$\mathbf{H}\left(\hat{\mathbf{s}}^{(n)}\right)\hat{\mathbf{s}}^{(n+1)} = \mathbf{A}^H\mathbf{y} \tag{9}$$

where n denotes the iteration number, and:

$$\mathbf{H}(\mathbf{s}) \triangleq 2\mathbf{A}^H\mathbf{A} + \alpha\Lambda(\mathbf{s}) \tag{10}$$

$$\Lambda(\mathbf{s}) \triangleq \operatorname{diag}\left\{ \frac{p}{(|\mathbf{s}_i|^2 + \epsilon)^{1-p/2}} \right\}$$

where $\operatorname{diag}\{\cdot\}$ is a diagonal matrix whose i-th diagonal element is given by the expression inside the brackets. The important difference from methods such as ridge regression lies in the dependence of $\Lambda(\mathbf{s})$ on the previous iterate, and on the use of a non-quadratic regularization term.

The method can also be interpreted as quasi-Newton with Hessian approximation $\mathbf{H}$. The full Hessian is given by

$$\nabla J_{\mathbf{ss}} = \mathbf{H}(\mathbf{s}) + \alpha \operatorname{diag}\left\{ \frac{p(p-2)|\mathbf{s}_i|^2}{(|\mathbf{s}_i|^2 + \epsilon)^{2-p/2}} \right\} \quad (11)$$

The second term is always negative and may make the Hessian indefinite. By keeping the first part only, we get a positive definite approximation to the Hessian. Also, for $p = 2$, the approximation becomes exact.

The quasi-Newton iteration has the following form:

$$\hat{\mathbf{s}}^{(n+1)} = \hat{\mathbf{s}}^{(n)} + \mathbf{H}\left(\hat{\mathbf{s}}^{(n)}\right)^{-1} \nabla J_{\mathbf{s}}\left(\hat{\mathbf{s}}^{(n)}\right) \quad (12)$$

By choosing stepsize to be equal to 1, a cancellation of the terms in the right hand side reduces this iteration to (9). We run the iteration until $\frac{\|\hat{\mathbf{s}}^{(n+1)} - \hat{\mathbf{s}}^{(n)}\|_2^2}{\|\hat{\mathbf{s}}^{(n)}\|_2^2} < \delta$, where $\delta > 0$ is a small constant. Compared to standard optimization tools, the above scheme yields an efficient method matched to the structure of our optimization problem. Convergence properties of algorithms of this type have been analyzed, and convergence from any initialization to a local minimum is guaranteed [4, 12].

4. CONDITIONS FOR UNIQUE SOLUTIONS

We shall limit this section solely to the consideration of the uniqueness of sparse representations of signals in terms of an overcomplete basis. The proposed method is an attempt to approximate the sparse representation, thus if the sparse representation is not unique then the proposed method will also have multiple possible solutions. However, the reverse is not always true. The question of uniqueness of global optima for cost function in (8), and the attainability of the unique sparse solution using the iterative procedure will not be considered.

Consider the inverse problem $\mathbf{y} = \mathbf{A}\mathbf{s}$, $\mathbf{y}$ is $M \times 1$, $\mathbf{A}$ is $N_\theta \times M$, and $\mathbf{s}$ is $N_\theta \times 1$. Using our representation, typically $\mathbf{A}$ will contain significantly more columns than the number of sensors, $N_\theta >> M$. Assuming that the array is rank-M unambiguos [17], every set of M distinct manifold vectors (columns of $\mathbf{A}$) will be linearly independent. Then any set of M columns form a basis for the space. If the number of sources $K \geq M$, sensor data can be represented by a linear combination of those K vectors, hence the representation is not unique. When $K < M$, a solution in terms of K arbitrary steering vectors will not exist for an arbitrary signal. However, if $K > M/2$, there will exist signals for which there are multiple possible sparse representations in terms of K steering vectors: consider a set of $2K$ array vectors $a_1, ..., a_{2K}$. If $2K > M$ then the set is linearly dependent, and there exist $\alpha_1...\alpha_{2K}$ such that $\sum_{i=1}^{K} \alpha_i a_i = \sum_{i=K+1}^{2K} \alpha_i a_i$. Any signal lying on the line $\gamma(\sum_{i=1}^{K} \alpha_i a_i), \gamma = -\infty..\infty$ will have two possible representations. The number of lines in the data space allowing ambiguous representations explodes combinatorially with the number of considered steering vectors, thus lack of

uniqueness becomes a likely outcome when even small amounts of noise are present. However, if $K \leq M/2$, then $\sum_{i=1}^{2K} \alpha_i a_i = 0$ only has the solution $\alpha_i = 0$ for all i. Therefore, the maximum number of sources with unique sparse representation in terms of an overcomplete rank-M unambiguous basis is $\lfloor (M+1)/2 \rfloor$. This conclusion corresponds well to the simulations. Note that we have not discussed whether the proposed approach will be able to arrive at the unique solution, thus this condition serves as an upper bound for the number of resolvable sources. For the beamspace version of the algorithm, the inverse problem is (6), and the situation gets more complicated, since rank of $\mathbf{V}$ has a nontrivial dependence on M. Simulations suggest that the upper bound on the number of resolvable sources is $M - 1$.

5. SIMULATION RESULTS

We presented the results for farfield narrowband case with uniform linear arrays and non-zero mean signals in [14]. First, we extend the results to zero-mean uncorrelated sources. A uniform linear array with 8 sensors is considered. We use $p = 0.1$ in our technique, and the regularization parameter is chosen by subjective assessment.
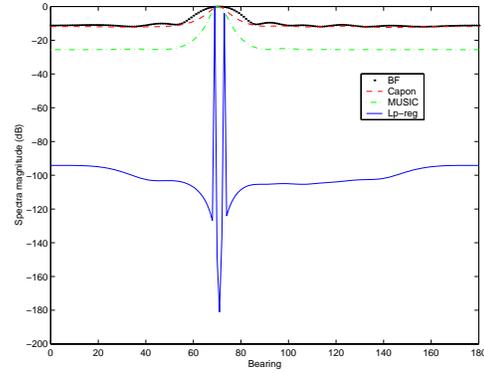
Fig. 1. Spatial spectra of two zero-mean sources with DOAs of $68°$ and $73°$. SNR = 0 dB.
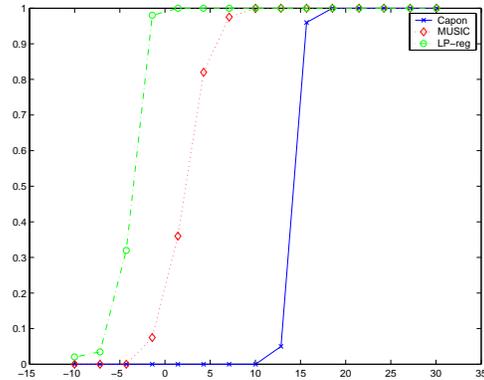
Fig. 2. Probability of correct detection as a function of SNR. DOAs: $68°$ and $73°$.

Figure 1 shows the spectrum plots with two sources coming from DOAS $68°$ and $73°$ from endfire. MUSIC, Capon's, and beamforming spectra fail to separate the peaks this close together and at such low SNR, whereas the proposed technique recovers both DOAs. Figure 2 examines the probability that the detected peaks fall within $1°$ of the true source location. The probability for each SNR is empirically obtained using 200 trials. It can be seen that the proposed technique performs better than the other techniques at low SNRs.

Next, we consider a nonlinear array geometry. No assumptions about linearity or uniformity of the array have been made in the development, thus the algorithm extends unchanged to any geometry. We consider an 8-element Mills cross array, with sensors residing on two perpendicular lines. We now consider non-zero mean signals, and the averaging version of the proposed technique. The cross array has a smaller spatial extent then the linear array with the same number of sensors, and thus the beamwidth is larger. To avoid dealing with asymptotic bias of the proposed technique [14], which occurs when the manifold vectors at the source DOAs are far from being orthogonal, the spacing between the signals is chosen to be $30°$. The spectrum plot is presented in Figure 3, and the probability of detection vs. SNR appears in Figure 4. The proposed technique performs better than MUSIC and Capon's methods at low SNR. The same behavior is observed for probability of detection vs. number of samples [14], thus the proposed technique is more robust to limited quantity and quality of sensor observations, provided that the steering vectors at the true source locations are sufficiently far from being linearly dependent.

Fig. 4. Probability of correct detection vs. SNR for Cross-array. DOAs: $60°$ and $90°$
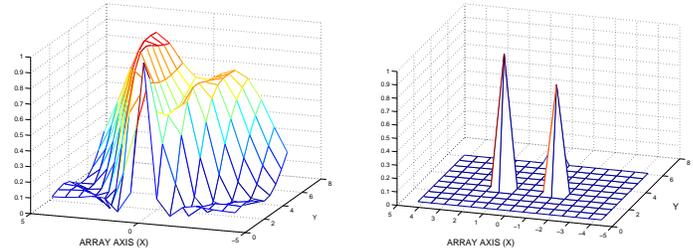
Fig. 5. Nearfield spectra: conventional (left) and proposed (right)

Fig. 3. Cross-array, two sources with DOAs of $60°$ and $90°$. SNR = 3 dB.

For the nearfield case, source locations are parameterized by range and bearing. By flattening the 2-D search grid into a vector we get a similar computational problem to that of the farfield case. The conventional and proposed reconstructions containing two nearfield narrowband sources are presented in Figure 5. The method exhibits resolution analogous to the farfield case. However, the dimension of the optimization problem grows quadratically with the fineness of the search grid. Thus to get very accurate estimates of the source locations tractably, either a multi-resolution approach or an approach separating the search variables has to be used.

The wideband case is accomplished in one of two ways. The most straightforward way is to process the data frequency by frequency, and to aggregate the resulting narrowband spectra. The amount of computation is proportional to the number of frequencies of interest. The conventional and proposed spectra for three chirps are presented in Figure 6. Note that when using the conventional method, the chirps are not resolved except at the very end of their frequency span.
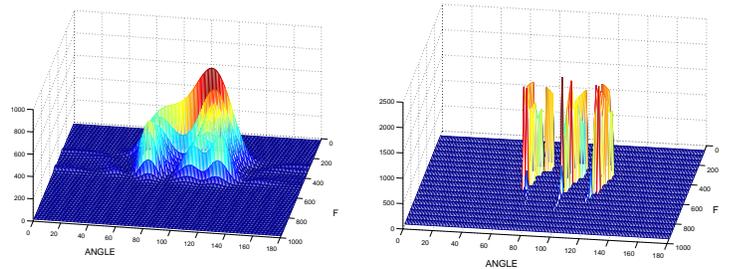
Fig. 6. Wideband spectra: conventional (left) and proposed (right)

The alternative way is to merge all frequencies into one model, and to reconstruct the resulting system once. One of the side-effects is that sparsity is enforced both spatially and in frequency. This enhances the resolution for signals consisting of multiple harmonics, but general wideband signals have to be treated differently. One possibility is to apply a different prior in the frequency domain, depending on the nature of the signals, for example on smoothness of the spectrogram. Another possibility is to use an appropriate basis

if the family of signals is restricted to have a sparse representation in that basis, for example, chirps have a sparse representation in the chirplet basis. Extension to the general wideband case is the subject of ongoing research.

6. CONCLUSIONS AND CURRENT WORK

We have approached the source localization problem with a sparse signal reconstruction perspective. We have developed and demonstrated the viability of a non-parametric superresolution source localization method in a variational framework, using ℓ_p-quasi-norm-based functionals as regularizing constraints. Several versions of the method have been presented to handle zero and non-zero mean signals, and correlated and uncorrelated sources. The approach improves upon the source localization accuracy of currently used nonparametric methods, especially in low-SNR and limited-data scenarios. The method is very versatile, encompassing farfield, nearfield, narrowband and wideband cases, as well as non-uniform array geometry.

Our current work involves the examination and extension of various aspects of our approach. An important issue in our method is the selection of the parameters p and α, which we have so far done manually based on subjective qualitative assessment. Developing techniques for automatic choice of these parameters is of great interest.

At the same time, we shall attempt to develop conditions for global convergence of the proposed method, and investigate the asymptotic bias in estimated source locations for closely spaced targets. Comparison of the iterative algorithm to other optimization methods such as the interior point methods also belongs to our agenda.

We are also working on developing extensions of our variational framework to handle self-calibration by taking into account uncertainties in sensor locations. As a starting point we are using a coordinate descent procedure optimizing the extended cost function alternatingly over source locations, and then over the sensor position errors.

7. REFERENCES

[1] J. Capon, "High resolution frequency-wavenumber spectrum analysis," *Proc. IEEE*, vol. 57, no. 8, pp. 1408–1418, 1969.

[2] R. O. Schmidt, "A Signal Subspace Approach to Multiple Emitter Location and Spectral Estimation," *Ph.D. thesis, Stanford Univ.*, Stanford, CA, 1981.

[3] C. R. Vogel and M. E. Oman, "Fast, robust total variation-based reconstruction of noisy, blurred images," *IEEE Trans. Image Processing*, vol. 7, no. 6, pp. 813–824, June 1998.

[4] P. Charbonnier, L. Blanc-Féraud, G. Aubert, and M. Barlaud, "Deterministic edge-preserving regularization in computed imaging," *IEEE Trans. Image Processing*, vol. 6, no. 2, pp. 298–310, Feb. 1997.

[5] M. Çetin and W. C. Karl, "Feature-enhanced synthetic aperture radar image formation based on nonquadratic regularization," *IEEE Trans. Image Processing*, vol. 10, no. 4, pp. 623–631, Apr. 2001.

[6] M. D. Sacchi, T. J. Ulrych, and C. J. Walker, "Interpolation and extrapolation using a high-resolution discrete Fourier transform," *IEEE Trans. Signal Processing*, vol. 46, no. 1, pp. 31–38, Jan. 1998.

[7] B. D. Jeffs, "Sparse inverse solution methods for signal and image processing applications," in *IEEE International Conference on Acoustics, Speech, and Signal Processing*, 1998, vol. 3, pp. 1885–1888.

[8] S. S. Chen, "Application of basis pursuit in spectrum estimation," in *IEEE International Conference on Acoustics, Speech, and Signal Processing*, 1998, vol. 3, pp. 1865–1868.

[9] S. Sibisi, J. Skilling, R. G. Brereton, E. D. Laue, and J. Staunton, "Maximum entropy signal processing in practical NMR spectroscopy," *Nature*, vol. 311, pp. 446–447, Oct. 1984.

[10] D. L. Donoho, I. M. Johnstone, J. C. Koch, and A. S. Stern, "Maximum entropy and the nearly black object," *J. R. Statist. Soc. B*, vol. 54, no. 1, pp. 41–81, 1992.

[11] D. Geman and G. Reynolds, "Constrained restoration and the recovery of discontinuities," *IEEE Trans. Pattern Anal. Machine Intell.*, vol. 14, no. 3, pp. 367–383, Mar. 1992.

[12] A. H. Delaney and Y. Bresler, "Globally convergent edge-preserving regularized reconstruction: an application to limited-angle tomography," *IEEE Trans. Image Processing*, vol. 7, no. 2, pp. 204–221, Feb. 1998.

[13] I. F. Gorodnitsky and B. D. Rao, "Sparse signal reconstruction from limited data using FOCUSS: a re-weighted minimum norm algorithm," *IEEE Trans. Signal Proc.*, vol. 45, no. 3, pp. 600-616, March 1997.

[14] M. Cetin, D. M. Malioutov, A. S. Willsky, "A variational technique for source localization based on a sparse signal reconstruction perspective," in *IEEE International Conference on Acoustics, Speech and Signal Processing*, Orlando, FL, USA, May 2002, vol. 3, pp. 2965–2968.

[15] W. J. Fu, "Penalized Regressions: the Bridge versus the Lasso," *Journal of Computational and Graphical Statistics*, Vol. 7, no. 3, September 1998.

[16] J. J. Fuchs "Linear Programming in Spectral Estimation. Application to array processing" in *IEEE International Conference on Acoustics, Speech and Signal Processing*, 1996, vol. 6, pp. 3161–3164.

[17] J. T. Lo, S. L. Marple, "Observability conditions for multiple signal direction finding and array sensor localization" *IEEE Trans. Signal Proc.*, vol. 40, no. 11, pp. 2641-2650, Nov. 1992.